

A Compact Channel-Dropping Filter for Stripline and Microwave Integrated Circuits

EDWARD G. CRISTAL, SENIOR MEMBER, IEEE, AND ULRICH H. GYSEL, MEMBER, IEEE

Abstract—A compact channel-dropping filter geometry is described that is particularly suited for stripline and microwave integrated circuits (MIC). The channel-dropping filter is comprised of a hairpin bandpass filter and a new bandstop filter, referred to herein as a folded-line bandstop filter. Design parameters for the latter filter for a range of bandwidths are tabulated. Analytical and experimental data for a trial channel-dropping filter are presented and discussed.

I. INTRODUCTION

MULTIPLEXERS are utilized to separate frequency bands from a spectrum of signals or to combine a number of frequency bands into a single spectrum. This can be accomplished using hybrids, circulators, and/or filters. A common technique is to cascade channel-dropping filters, each of which separates or combines a particular band of frequencies. Each channel-dropping filter consists of a bandpass and a bandstop filter suitably designed and interconnected to produce a constant-resistance input impedance.

The theory for constant-resistance channel-dropping filters has been described by several authors, and no new theory is presented in this paper [1]–[3]. What we are concerned with here is the feasibility of a new channel-dropping-filter geometry that is particularly compact and that utilizes the stripline or microwave integrated circuit (MIC) surface area in a highly efficient manner. Channel-dropping filters often consist of interdigital, combline, or half-wave parallel coupled-line bandpass filters combined with bandstop filters consisting of quarter-wavelength stubs separated by quarter-wavelength lines—i.e., unit elements [4]. For example, a channel-dropping filter in stripline consisting of a half-wave parallel coupled-line bandpass filter and quarter-wavelength-line bandstop filter might take the Y form shown in Fig. 1(a) or the T form¹ shown in Fig. 1(b). On the other hand, the channel-dropping filter geometry described in this paper utilizes compact hairpin bandpass and folded-line bandstop filters. A configuration analogous to those shown in Figs. 1(a) and (b), utilizing the latter filters and on the same scale,

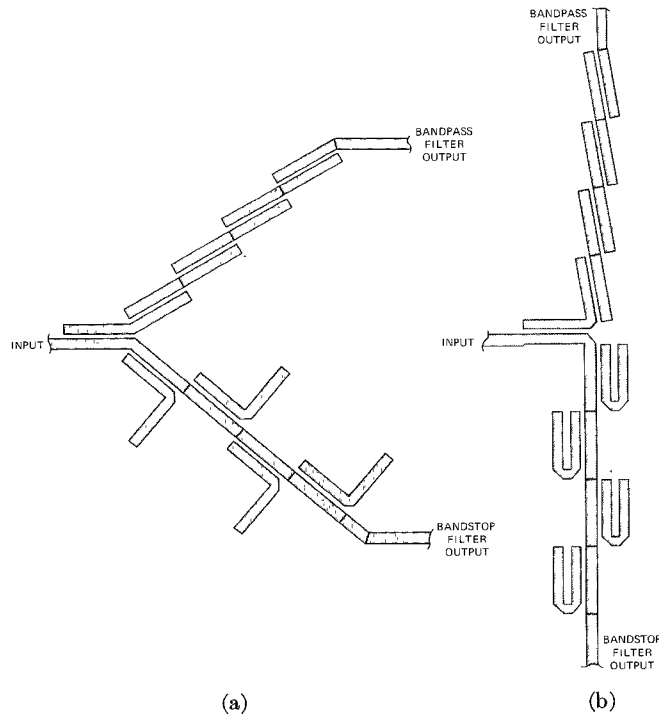


Fig. 1. Stripline channel-dropping filters utilizing half-wave parallel coupled-line bandpass filters and quarter-wavelength-line bandstop filters. (Figs. 1 and 2 are drawn to the same scale.)

is shown in Fig. 2. It is quite clear from the figure that the new geometry utilizes the surface area of the substrate very effectively. In addition, the relative efficiency increases as the number of filter resonators increases. Lastly, use of hairpin and folded-line filters permits numerous hybrid geometries for increased design flexibility [5], [6].

Two methods for designing the individual filters of a channel-dropping filter are the following. 1) Use approxi-

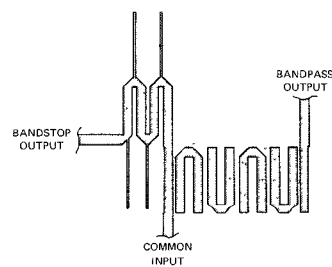


Fig. 2. Compact stripline channel-dropping filter utilizing hairpin bandpass filter and folded-line bandstop filter. (Figs. 1 and 2 are drawn to the same scale.)

Manuscript received August 6, 1973; revised January 10, 1974. This work was supported by the U. S. Army Electronics Command, Fort Monmouth, N. J., under Contract DAAB07-72-C-0127.

E. G. Cristal is with the Hewlett-Packard Laboratories, Palo Alto, Calif.

U. H. Gysel is with the Stanford Research Institute, Menlo Park, Calif. 94025.

¹ Suggested by one of the reviewers.

mate methods and singly terminated prototypes. 2) Use exact transfer functions for singly terminated filters and modern synthesis methods. The hairpin bandpass filter can be designed via either of these methods [5], [6]. However, for the folded-line bandstop filter, no conventional synthesis methods exist at the present time. Consequently, a numerical optimization method was selected for the compilation of design tables. A numerical optimization method had the additional advantage that the coupling between folded lines, as well as the stub impedances, could be easily restricted to reasonable values prior to the start of the filter design. Thus physical realizability was guaranteed from the outset.

II. FILTER DESIGN CONSIDERATIONS

A. Folded-Line Bandstop Filter

The general form for the folded-line bandstop filter is given in Fig. 3. Its equivalent circuit can be obtained by appropriately adding stubs to the equivalent circuit for meander lines given by Sato [7]. This is shown in Fig. 4. Coupling between folded lines is accounted for solely by "S-plane inductors" connecting unit elements. In Fig. 4, unit elements are depicted as straight lines, and short-circuited stubs as inductors. An "unfolded" conventional bandstop filter is obtained by setting all inductive admittance values to 0. A hybrid geometry is obtained by setting some but not all inductive admittance values to 0. Using the equivalent circuit of Fig. 4, the network response of the folded-line bandstop filter can be calculated for use in various numerical optimization

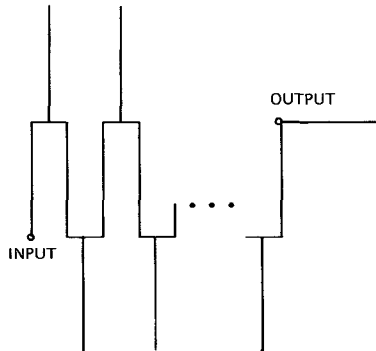


Fig. 3. Folded-line bandstop filter.

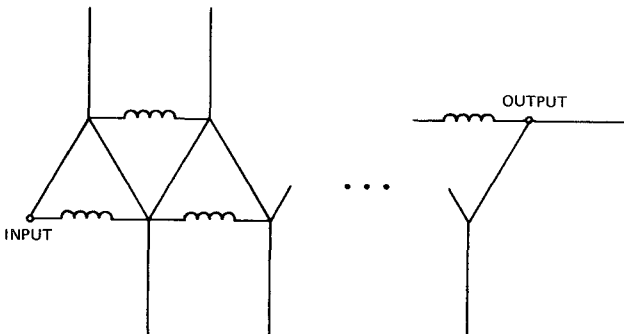


Fig. 4. Folded-line bandstop-filter equivalent circuit.

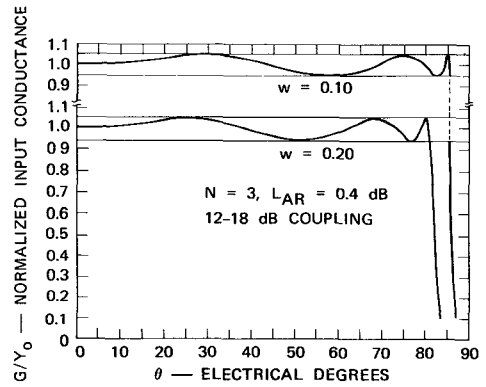


Fig. 5. Calculated normalized input conductance for two folded-line bandstop filters.

programs. The authors utilized a least p th minimization algorithm that maximized the selectivity and forced an equi-ripple response in the passband.

Two typical results of the optimization program are shown in Fig. 5. These curves are normalized input conductances of two singly terminated commensurate-length bandstop filters consisting of three unit-elements and three stubs for equi-ripple bandwidths of 10 and 20 percent and 0.4-dB ripple.² Note that the curves deviate equally above and below the load value. This was done to optimize the VSWR of the channel-dropping filter [1], [2]. The curves have the maximum number of extremes and are equi-ripple for practical purposes.

The selectivity of folded-line bandstop filters was compared with the selectivity of the corresponding optimum unfolded filter, and it was found that they were essentially the same. However, this may only hold for the range of couplings used in this paper (i.e., -12 to -18 dB).

B. Bandstop Filter Design Tables

Fig. 6 is a cross-sectional representation of an arbitrary coupled transmission-line network in any TEM or quasi-TEM medium, and depicts the unnormalized distributed capacitance parameters C_{g_i} and $C_{i,i+1}$. These are defined as follows:

$$C_{g_i} = \text{Capacitance to ground per unit length for the } i\text{th conductor}$$

$$C_{i,i+1} = \text{Mutual capacitance per unit length between the } i\text{th and } (i+1)\text{th conductors.} \quad (1)$$

Coupling between nonadjacent lines is assumed negligible.

The dimensionless distributed-capacitance parameters that are needed for use with Getsinger's data [8] in order to obtain dimensional parameters from electrical parameters are as follows:

$$c_{g_i} = C_{g_i}/\epsilon$$

$$c_{i,i+1} = C_{i,i+1}/\epsilon$$

$$\epsilon = \epsilon_r \epsilon_0$$

² 0.4-dB ripple corresponds to $G_{\max}/G_{\min} = 1.0965$.

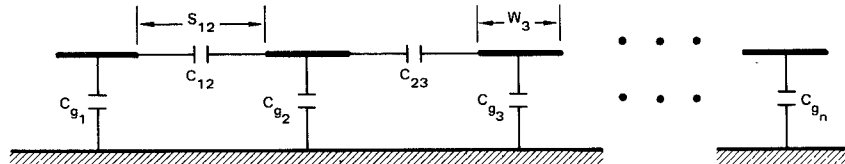


Fig. 6. Schematic cross-sectional representation for coupled transmission lines.

TABLE I
THREE-SECTION MEANDER-LINE SINGLY TERMINATED BANDSTOP-FILTER CAPACITANCES NORMALIZED TO $376.7/(\epsilon_r)^{1/2}$ *
COUPLING = -12.0 TO -18.0 dB; PASSBAND RIPPLE = 0.400 dB

w	w_3 dB	CG1/ε	CG2/ε	CG3/ε
0.025	0.02113	0.8338	0.7300	0.8877
0.050	0.04211	0.8253	0.7103	0.8684
0.075	0.06386	0.8500	0.7578	0.8920
0.100	0.0857	0.7880	0.6729	0.8472
0.125	0.1081	0.8138	0.7317	0.8875
0.150	0.1298	0.8251	0.6877	0.8154
0.175	0.1523	0.8562	0.7193	0.8104
0.200	0.1751	0.8056	0.6902	0.8215

w	w_3 dB	CM12/ε	CM23/ε
0.025	0.02113	0.1793	0.1476
0.050	0.04211	0.1788	0.1562
0.075	0.06386	0.1338	0.1154
0.100	0.0857	0.2015	0.1529
0.125	0.1081	0.1550	0.9311E-01
0.150	0.1298	0.1300	0.1607
0.175	0.1523	0.7865E-01	0.1463
0.200	0.1751	0.1222	0.1229

w	w_3 dB	YSTUB1	YSTUB2	YSTUB3
0.025	0.02113	0.1774E-01	0.2073E-01	0.1499E-01
0.050	0.04211	0.3570E-01	0.4042E-01	0.2956E-01
0.075	0.06386	0.5903E-01	0.6644E-01	0.4481E-01
0.100	0.0857	0.7027E-01	0.8295E-01	0.5975E-01
0.125	0.1081	0.9677E-01	0.1183	0.7658E-01
0.150	0.1298	0.1230	0.1230	0.8904E-01
0.175	0.1523	0.1605	0.1479	0.1058
0.200	0.1751	0.1690	0.1795	0.1222

* The numbering of the table values starts at the diplexer junction of the folded-line bandstop filter.

ϵ_r = Relative dielectric constant of the medium

ϵ_0 = Permittivity of free space in the units of C_{gi} and $C_{i,i+1}$. (2)

The coupling $k_{i,i+1}$ between folded unit elements i and $i+1$ is defined as

$$k_{i,i+1} = 20 \log_{10} \frac{C_{i,i+1}}{[(C_{gi} + C_{i,i+1})(C_{g,i+1} + C_{i,i+1})]^{1/2}} \text{ dB.} \quad (3)$$

The fractional bandwidth of the bandstop filter is defined as

$$w = (f_2 - f_1)/f_0 \quad (4)$$

where f_2 and f_1 are the upper and lower equi-ripple stopband-edge frequencies, respectively, and f_0 is the center frequency of the stopband.

Design parameters for folded-line bandstop filters are

TABLE II
FIVE-SECTION MEANDER-LINE SINGLY TERMINATED BANDSTOP-FILTER CAPACITANCES NORMALIZED TO $376.7/(\epsilon_r)^{1/2}$ *
COUPLING = -12.0 TO -18.0 dB; PASSBAND RIPPLE = 0.400 dB

w	w_3 dB	CG1/ε	CG2/ε	CG3/ε	CG4/ε	CG5/ε
0.025	0.02345	0.8866	0.7119	0.6707	0.7579	0.9218
0.050	0.04674	0.8726	0.7574	0.7171	0.7436	0.9058
0.075	0.07068	0.8540	0.7258	0.6947	0.7331	0.8959
0.100	0.09453	0.8566	0.7154	0.6928	0.7109	0.8475
0.125	0.1184	0.8412	0.7134	0.7027	0.7240	0.8577
0.150	0.1426	0.8332	0.7154	0.7132	0.7001	0.8213
0.175	0.1660	0.8240	0.6904	0.6969	0.6900	0.8020
0.200	0.1902	0.8158	0.7071	0.7146	0.7190	0.8307

w	w_3 dB	CM12/ε	CM23/ε	CM34/ε	CM45/ε
0.025	0.02345	0.1138	0.2302	0.1877	0.1161
0.050	0.04674	0.1146	0.1392	0.1827	0.1170
0.075	0.07068	0.1250	0.1515	0.1790	0.1123
0.100	0.09453	0.1086	0.1630	0.1487	0.1534
0.125	0.1184	0.1099	0.1354	0.1342	0.1242
0.150	0.1426	0.1084	0.1186	0.1201	0.1521
0.175	0.1660	0.1054	0.1329	0.1052	0.1591
0.200	0.1902	0.1006	0.9689E-01	0.9902E-01	0.1095

w	w_3 dB	YSTUB1	YSTUB2	YSTUB3	YSTUB4	YSTUB5
0.025	0.02345	0.2297E-01	0.2215E-01	0.2372E-01	0.2418E-01	0.1600E-01
0.050	0.04674	0.4609E-01	0.5267E-01	0.4794E-01	0.4827E-01	0.3175E-01
0.075	0.07068	0.6854E-01	0.7739E-01	0.7275E-01	0.7364E-01	0.4802E-01
0.100	0.09453	0.9541E-01	0.1012	0.1030	0.9099E-01	0.6330E-01
0.125	0.1184	0.1188	0.1326	0.1325	0.1202	0.8012E-01
0.150	0.1426	0.1450	0.1664	0.1648	0.1374	0.9721E-01
0.175	0.1660	0.1704	0.1872	0.1978	0.1562	0.1120
0.200	0.1902	0.1977	0.2327	0.2292	0.1989	0.1265

presented in Tables I and II, for $N = 3$ and 5 , $w = 0.025$ to 0.20 in steps of 0.025 , and a passband ripple of 0.4 dB. Self- and mutual capacitances are listed under the column headings CGi/ϵ and $CMij/\epsilon$, respectively. These values may be converted to the dimensionless forms C/ϵ required by Getsinger's data, by the equation

$$\left. \begin{aligned} C_{gi}/\epsilon \\ \text{or} \\ C_{i,i+1}/\epsilon \end{aligned} \right\} = \frac{376.7}{RL(\epsilon_r)^{1/2}} \{ \text{Table I or II value} \} \quad (5)$$

where RL is the load resistance in ohms. The normalized stub admittances are listed under the column heading YSTUB1. The unnormalized stub admittances are given by

$$Y_i(\text{STUB}) = \frac{1}{RL} \{ \text{Table I or II value} \}. \quad (6)$$

An additional parameter, listed in Tables I and II under the heading w_3 dB is the 3-dB fractional bandwidth

of the bandstop filters. This bandwidth is defined as $(f_2' - f_1')/f_0$, where f_1' and f_2' are the frequencies at which the normalized conductance equals 0.5 and f_0 is as before. This value is needed to find the proper bandwidth of the quasicomplementary hairpin-line bandpass filter.

For the data presented in Tables I and II the coupling between meander-line turns was arbitrarily required to be within the range -12 to -18 dB. This range of coupling generally yields a realizable and compact structure for coplanar coupled strips. The impedance of the transmission-line stubs of the bandstop filters may be too large to realize directly. In those cases, capacitive-coupled "half-wave" open-circuited stubs can be substituted. The impedance of the half-wave lines may be set to a reasonable value (e.g., 100Ω), and the coupling capacitors and line lengths adjusted to give the correct resonance and slope parameter.

C. Hairpin Bandpass Filter

To build a channel-dropping filter, the bandstop filter has to be complemented (or quasicomplemented) by a bandpass filter, in this case a hairpin or hybrid-hairpin filter. The existing design procedures may be used [5], [6], but the prototype filter should be singly terminated. Also, if a Chebyshev prototype is used, the equi-ripple bandwidth should be adjusted so that the normalized conductances of the bandpass and bandstop filters cross over at approximately 0.5.

In general, when the two filters are equi-ripple, they can only be quasicomplementary. This will result in a variation of the VSWR at the common junction, particularly in the vicinity of crossover. An additional factor can adversely effect the VSWR when a hairpin bandpass filter is used. Analytical studies, supported by computer calculations, show that the common input is directly coupled to the interior of the bandpass filter via the first hairpin resonator. Fortunately, however, the coupling can be reduced to negligible values by reducing the internal coupling of the first hairpin resonator³ to about -20 dB or less.

Fig. 7 shows the calculated attenuations and common-port VSWR of an example channel-dropping-filter design.

III. EXPERIMENTAL RESULTS

In order to experimentally verify the bandstop-filter design, a separate bandstop filter with the following specifications⁴ was constructed and tested: a) equi-ripple bandwidth = 0.10; b) ripple = 1.0 dB ($G_{\max}/G_{\text{load}} = 1.256$); c) coupling between folded lines = -16 to -20 dB; d) center frequency = 1.5 GHz; e) three unit elements; f) three stubs.

A singly terminated hairpin filter was also designed with

³ The internal coupling of a hairpin resonator is the coupling between the two lines constituting the resonator.

⁴ These experimental tests were made at an intermediate stage of this project prior to the completion of the final computer program. The bandstop filter design selected was not equiripple but was judged sufficiently good to test the feasibility of channel-dropping-filter design.

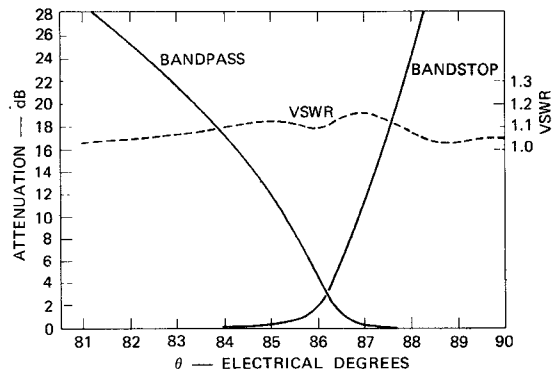


Fig. 7. Calculated attenuation and VSWR at common port of optimally designed multiplexer ($N = 3$, 0.4-dB ripple; equi-ripple bandwidth: $w_{\text{BS}} = 0.1$, $w_{\text{BP}} = 0.071$; coupling of first hairpin = -24 dB, all other couplings = -16 dB).

a slightly smaller equi-ripple bandwidth in order to obtain crossovers of the conductance curve at 0.5 normalized values. The filters were constructed in stripline in Rexolite 1422 ($\epsilon_r = 2.54$) with ground-plane spacing of 0.250 in. The admittances of the bandstop-filter stubs were too small to realize directly. Hence, capacitive coupled half-wave stubs were substituted. American Technical Ceramics capacitor chips were used as coupling capacitors for the half-wave lines. The design specifications for the two filters are given in Table III. The channel-dropping filter is shown in Fig. 8.

The normalized input conductance of the folded-line bandstop filter was experimentally measured. The data are given in Fig. 9 along with the theoretically computed result. It is seen that the bandwidth of the trial filter is a little greater than theoretical, but that there is fairly good agreement between the two curves. The increase in the measured bandwidth of the trial filter is most likely due to too small a slope parameter for the shunt stubs and could be adjusted by reducing the capacitive coupling of the half-wave resonators. The hairpin filter was also measured by itself and was found to have the proper admittance characteristic, although the bandwidth was slightly narrow relative to the bandwidth of the bandstop filter. However, it was decided to make corrective adjustments after the filters were connected.

Next, the bandpass and bandstop filters were connected and tuned. Initial measurements of return loss and attenuation of the bandpass and bandstop verified that the bandpass-filter bandwidth was too small. This was corrected by decreasing the spacing between the second and third resonators of the hairpin filter. The final responses after tuning are given in Fig. 10. The return loss was quite good below and throughout the passband, but deteriorated to around 13 dB from 1.8 to 2.0 GHz. Above 2 GHz the return loss continued to deteriorate and was only 10 dB at 2.3 GHz. There were several factors contributing to this: a) the relatively large ripple of the prototype (1.0 dB); b) incomplete compensation of the interconnections of the hairpin resonators and folded lines; and c) the use of capacitive-coupled half-wave resonators in the bandstop filter. In the case of the present trial

TABLE III
INITIAL PARAMETERS VALUES FOR TRIAL CHANNEL-DROPPING FILTER

Hairpin Filter						
i	C_g/ϵ	C_m/ϵ^*	W/H^\dagger	S/H^\dagger	W (inch)	S (inch)
1	3.6280	1.6054	0.6474	0.0625	0.1619	0.0156
2	3.3569	0.1293	0.6111	0.7401	0.1528	0.1850
3	4.0196	0.5020	0.6823	0.3246	0.1706	0.0811
4	4.2664	0.1249	0.7427	0.7511	0.1857	0.1878
5	4.1919	0.6015	0.7385	0.2740	0.1846	0.0685
6	3.8289	0.1334	0.6502	0.7303	0.1625	0.1826
7	3.0802	2.0121	0.5557	0.0357	0.1389	0.0089
8	3.4899		0.6255		0.1564	

Folded-Line Bandstop Filter						
i	C_g/ϵ	C_m/ϵ	W/H	S/H	W (inch)	S (inch)
1	4.2975	0.5852	0.7324	0.2815	0.1831	0.0704
2	3.5482	0.5748	0.6582	0.2865	0.1645	0.0716
3	4.1514		0.6946		0.1737	

Bandstop-Filter Normalized Stub Admittance						
i		Y_s/Y_0^\dagger				
1		0.08229				
2		0.08010				
3		0.05626				

* $C_m = C_{i,i+1}$

S = Strip-to-strip spacing

† H = Ground-plane spacing

W = Strip width

‡ Y_0 = Generator admittance; Y_s = Stub admittance

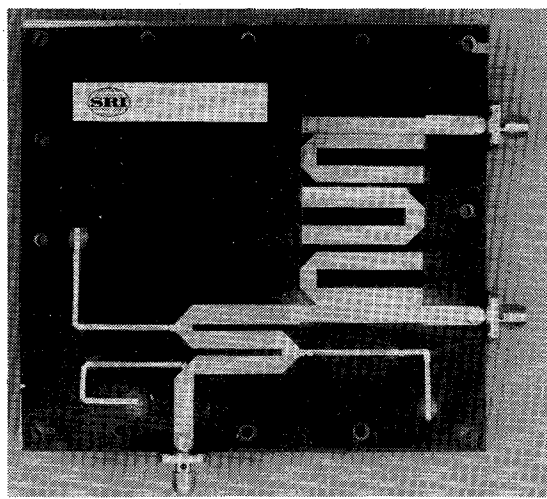


Fig. 8. Trial channel-dropping filter.

channel-dropping filter, the latter cause was the most dominant.

The 3-dB bandwidth of the dropped channel measured 10.2 percent. The midband loss was 1.5 dB and the crossovers occurred at 6 and 7 dB.

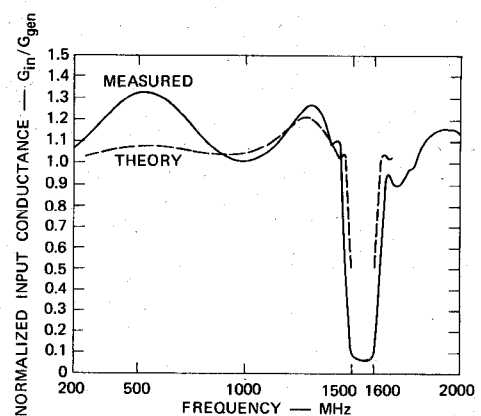


Fig. 9. Theoretical and experimental normalized input conductance of trial folded-line bandstop filter.

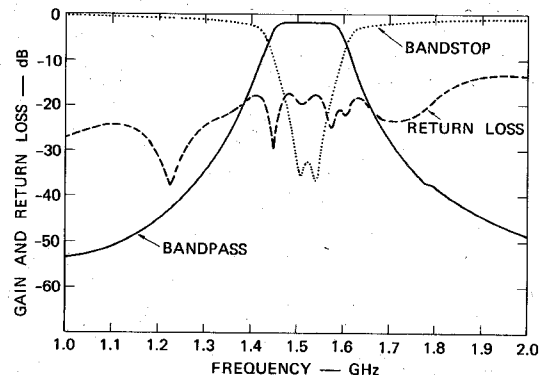


Fig. 10. Return loss and gain of final channel-dropping filter.

IV. CONCLUSIONS

Design tables have been presented for folded-line bandstop filters for use in channel-dropping filters. The bandstop filters are equi-ripple and have very similar electrical characteristics to unfolded optimum bandstop filters of the same order.

The measured input conductance of a trial bandstop filter compared favorably with the theoretically computed curve. Discrepancies were attributed to inadequate compensation of the interconnections between folded lines, and to the effect of the substitutions of capacitive-coupled half-wave resonators for the high-impedance quarter-wavelength stubs. The trial channel-dropping filter was judged to verify the design procedure and the feasibility of the new compact geometry for stripline and MIC. However, the use of half-wave coupled resonator stubs caused degradation of return loss above the passband. The latter effect could be a serious drawback to the design approach if a large number of channels are to be cascaded or for applications at higher frequencies. However, a compromise could be achieved by using hybrid forms for the folded-line filter or, finally, a totally conventional linear bandstop filter at a cost in physical compactness.

REFERENCES

- [1] G. L. Matthaei and E. G. Cristal, "Theory and design of diplexers and multiplexers," in *Advances in Microwaves*, vol. 2, Leo Young, Ed. New York: Academic, 1967.

- [2] R. J. Wenzel, "Application of exact synthesis methods to multi-channel filter design," *IEEE Trans. Microwave Theory Tech. (1964 Symposium Issue)*, vol. MTT-13, pp. 5-15, Jan. 1965.
- [3] —, "Printed-circuit complementary filters for narrow bandwidth multiplexers," *IEEE Trans. Microwave Theory Tech.*, vol. MTT-16, pp. 147-157, Mar. 1968.
- [4] H. Ozaki and J. Ishii, "Synthesis of transmission-line networks and the design of UHF filters," *IRE Trans. Circuit Theory*, vol. CT-2, pp. 325-336, Dec. 1955.
- [5] E. G. Cristal and S. Frankel, "Hairpin-line and hybrid hairpin-line/half-wave parallel-coupled-line filters," *IEEE Trans. Microwave Theory Tech.*, vol. MTT-20, pp. 719-728, Nov. 1972.
- [6] U. H. Gysel, "New theory and design for hairpin-line filters," this issue, pp. 523-531.
- [7] R. Sato, "A design method for meander-line networks using equivalent circuit transformations," *IEEE Trans. Microwave Theory Tech.*, vol. MTT-19, pp. 431-442, May 1971.
- [8] W. J. Getsinger, "Coupled rectangular bars between parallel plates," *IRE Trans. Microwave Theory Tech.*, vol. MTT-10, pp. 65-73, Jan. 1962.

The Effect of Cross-Section Curvature on Attenuation in Elliptic Waveguides and a Basic Correction to Previous Formulas

LEONARD LEWIN, ASSOCIATE MEMBER, IEEE, AND ALI M. B. AL-HARIRI

Abstract—It is shown that a certain asymptotic expansion of the Mathieu function of the fourth kind has almost certainly been inappropriately applied to previous elliptic waveguide calculations. An appropriate expansion is discussed at some length, and leads to a substantial modification of the published formulas. The need for a correction is demanded by a physical requirement to give the limit of the conventional surface impedance expression at the broad face of a very elongated elliptical shape.

A curvature effect, the subject of some recent technical discussions, survives the change, and a discussion is given of an unsuccessful attempt to create a generalized form that replaces the ellipse parameters by differentials of the local curvature of the surface. An attempt is also made to justify the reality of such a substantial curvature effect. However, no effect occurs for flat surfaces or those of uniform curvature, confirming the validity of the usual perturbation technique of calculating waveguide attenuation in those cases.

An anomalous property of the characteristic numbers of the Mathieu functions is discussed insofar as it relates to the present problem.

I. INTRODUCTION

RECENT papers [1]-[3] have drawn attention to a position-dependent curvature contribution to the attenuation coefficient of elliptic waveguides. If the attenuation is calculated according to the familiar perturbation method, which applies adequately to parallel plate and circular waveguides, both of which can also be

Manuscript received August 6, 1973; revised October 19, 1973. This work was supported in part by a grant from the Science Research Council.

L. Lewin was with the Department of Electrical Engineering, Queen Mary College, University of London, London, England, on leave during 1973 from the Department of Electrical Engineering, University of Colorado, Boulder, Colo. 80302.

A. M. B. Al-Hariri is with the Department of Electrical Engineering, Queen Mary College, University of London, London, England.

analyzed on a rigorous basis, the result does not agree with the classic computation of Chu [4]. It is necessary, in order to get agreement, to specify a longitudinal and a transverse surface impedance, both of which depend on position round the guide [1].

The concept of a surface impedance depending on position and exhibiting anisotropy for an isotropic wall material is a little surprising, and in the process of a thorough checking of the formulas, it was discovered that they led to an unacceptable form in the limiting case of a very elongated ellipse. If $2a$ and $2b$ are the major and minor axes, e the ellipticity, η the azimuthal elliptic coordinate, and Z_{s0} the surface impedance for an isotropic flat surface, then the calculations indicate an axial and transverse surface impedance for elliptic guide of values [1]

$$Z_a = Z_{s0}(1 - e^2 \cos^2 \eta)^{1/2}(a/b) \quad (1)$$

$$Z_t = Z_{s0}(1 - e^2 \cos^2 \eta)^{-1/2}(b/a). \quad (2)$$

For fixed b , and $a \rightarrow \infty$, (1) gives $Z_a \rightarrow \infty$, which must be wrong, since the region around $\eta = \pi/2$ clearly represents part of a parallel plate guide with $Z_a = Z_{s0}$.

This paper examines the cause of the discrepancy and attempts a qualitative description of the cause of the curvature effects, as well as a generalization to nonelliptic shapes.

II. MODIFIED ATTENUATION FORMULAS

A. Mathieu Function Asymptotic Forms

In the metal wall we are concerned with Mathieu functions of the fourth kind (analogous to outgoing